CFD study of thermal effect on Power-law fluid in rotating annular flow

by

Mahmoud Tarek Mahmoud Ali Shahin
15826

May 2015

Universiti Teknologi PETRONAS
Bandar Seri Iskandar
31750 Tronoh
Perak Darul Ridzuan

CERTIFICATION OF APPROVAL

CFD study of thermal effect on Power-law fluid in rotating annular flow

By

Mahmoud Tarek Mahmoud Ali Shahin

A project dissertation submitted to the
Petroleum Engineering Programme
Universiti Teknologi PETRONAS
In partial fulfilment of the requirement for the
BACHELOR OF ENGINEERING (Hons)
PETROLEUM

Approved by

____

(Titus Ntow Ofei)

UNIVERSITI TEKNOLOGI PETRONAS
TRONOH, PERAK
May 2015

CERTIFICATION OF ORIGINALITY

This is to certify that I am responsible for the work submitted in this project, that the original work is my own except as specified in the references and acknowledgements, and that the original work contained herein have not been undertaken or done by unspecified sources or persons.

Mahmoud Tarek mahmoud Ali shahin

Abstract

Drilling in oil and gas industry is a crucial and precarious process. Inaccurate estimation or expectation of any of the parameters interfering in this process can lead to catastrophic results if not handled carefully and in proper timing. One of the main parameters is the drilling fluid, which is used throughout the whole drilling procedure for numerous functions. The drilling fluid is tested under normal atmospheric temperature. However in the drilling process the fluid is exposed to high temperature that can impact the drilling fluid properties and flow behavior. Adding to that the rotation of the drill string impact which can change the dynamic viscosity of the fluid. As more high temperature high pressure wells are being drilled the need to better understand the impact of high temperature in the fluid annular flow became necessary. In this study we tried to understand and investigate the effect of both temperature and rotation on the properties of the drilling fluid and on the flow behavior in a concentric annuli. The scope and methodology of this research involved Computational Fluid Dynamics (CFD) approach, with ANSYS-CFX (in ANSYS 15) as the analysis system, where a CFD model with an optimum mesh size was created and validated against previous experimental data. The fluid was modelled using Power Law rheology. A vertical wellbore with a concentric and rotating drill-string was considered where the fluid flow was assumed laminar, steady state and fully developed. Different rotation speeds and temperatures points were selected to measure the different responses against changing these parameters. Rotation speeds of 0, 60,120,180,220 RPMs and temperatures of 298 K,323 K ,373 K and 423 K were selected and the simulated. Results from these simulations show that rotation combined with high temperature significantly affects both dynamic viscosity and coupled velocity in the annulus. We notice the effect of rotation on the distribution of heat through the annulus closer to the outer wall the temperature at static condition is higher than at 220RPM and at 220 the temperature is dropping faster than at static condition. However in the middle of the annulus both profiles seem symmetric and moving at same rate. Near the rotation the temperature is dropping slower at 220 RPM due to the rotation that helps to distribute the heat, unlike the case in static conditions. This also impact the dynamic viscosity which is decreasing with higher rotation speed and leading to increase in velocity. These results will help researchers and actual field engineers to better understand the drilling fluid changes in high temperature wells while the drilling process is ongoing with rotating drill-string.

Acknowledgement

The author would like to express utmost gratitude to Mr Titus Ntow Ofei who never stopped guidance and help throughout the entire study. He was generous with his expertise and time and provided continuous support and encouragement that greatly assisted in the completion of this study.

In addition I would like to thank Mr Asif zamir who was very understanding coordinator and helped us to follow the time schedule and interfered where necessary.

Last but not least, the author wishes to show his appreciation to all parties involved in this project and those who helped to complete this study.

TABLE OF CONTENTS

Contents

Abbreviation and nomenclature

CFD: Computation Fluid Dynamics

RPM: Rotation per Minute

ID: Inner Diameter

OD: Outer Diameter

HTHP: High Temperature High Pressure

CHAPTER 1

INTRODUCTION

1.1 Project Background

In the last few years many extensive Computational fluid dynamics (CFD) studies have been conducted on thermal effect on power law fluids due to their large applications in the industry and the engineering process such as the food industries, plastic manufacturing, pharmaceutical products, cosmetics, glass fiber and paper production and drilling mud manufacturing. Few researchers and scientists have focused on the power law fluids used on the drilling fluids and the thermal effect on their flow. Also the behavior of power law fluids in rotation condition and the rheology of these fluids under different conditions of rotation and either turbulent or laminar flow have been analyzed.

However few Studies by Manglik et all (2002) have been conducted to study the combined effect of both rotation and thermal changes on the fluid behavior. This study will focus on the thermal effect on the power law fluid in rotating annular flow. A good example is the circulation process of mud in oil and gas wells. To achieve a number of functions that help in the drilling process, the drilling mud which is a non-Newtonian fluid flows down through the drill string and then up through the annular space between the drilling string and the rock formation. The space between the drilling string and the rock formation is called the annulus. The drilling fluid must meet certain criteria to guarantee the ease and continuity of a drilling operation.

The characteristics of the drilling mud such as the density, gel strength, plastic viscosity and mud weight should be calculated carefully. Any inaccuracy in the measurement of these characteristics will result in premature production of formation fluid which is known in the drilling industry as a kick. Also we need a high shear thinning strength to ensure the drilled cuttings can be carried at low pumping power. Since most of these characteristics are functions of heat, our results would be inaccurate if we considered the entire well to be at uniform temperature. The heat effect on the drilling fluid can change most of its measured characteristics.

The properties of the drilling flow in the annulus can change due to the thermal effect which may or may not lead to great change in their flow behavior in the annulus. Two scenarios can happen in this condition, firstly there is rotation and secondly there is no rotation. In this study the first scenario will be addressed and the study will be conducted assuming a rotational flow in the annulus.

1.2. Problem Statement

During drilling operation there is always heat transfer from the rock formation to the drilling fluid. This impact will lead to heat interaction with the drilling fluid circulating in the well bore thus influence the flow dynamics of the fluid and its rheology. However most drilling fluids are designed under atmospheric conditions before circulation begins. Thus the fluid undergoes different flow and rheological changes when it experiences down hole conditions. The combined effect of head and drill pipe rotation on the flow dynamics and fluid rheology are important phenomena that needs to be understood during drilling operations. This phenomenon will further explain the cuttings carrying behavior of the drilling fluid.

1.3. Objective

The objectives of this study are as follows:

- To analyze the thermal and drill string rotation effects on the dynamic viscosity and velocity of the drilling fluid annular flow.

- To predict the flow patterns in the annular region due to the effect of heat and drill string rotation.

- To find and generate a relationship between the fluid flow changes and temperature changes and rotation changes.

1.4. Scope of Study

The scope of this study will cover the following aspects:

- A vertical concentric annulus is considered with the fluid flow obeying the power-law fluid model.
- The flow is considered laminar, steady state fully developed and non-isothermal, with the fluid as incompressible.
- A commercial software, ANSYS, will be used to model the flow geometry, whereas, the flow equations will be solved using CFX solver.

CHAPTER 2

LITERATURE REVIEW

2.1 Fluid type and pattern effect on heat transfer

Many studies and researches have shown that the type of fluid and its flow can affect heat transfer gradients. These parameters can change dramatically the heat transfer to the fluid and hence can change the expected impact of heat on that fluid.

As Manglik (2002) results show that different fluids exhibit different responses to the heat transfer.

For laminar flow in a concentric annulus Manglik (2002) results show that shear thinning fluids are likely to have marginally more wall temperature gradients due to their plug flow behavior. However on the other hand shear thickening fluids have less wall temperature gradient due to their conical flow. This effect is greatly altered in eccentric annulus. However in dilatant fluids that have higher peak velocities close to pseudo plastic fluids a higher mid-plane temperatures are observed even with change in eccentricity.

Manglik comments on his results for the effect of eccentricity in the same research that eccentricity can lead to mobility reduction leading to different heat transfer effects, however for a concentric annuli or semi concentric the flow mobility is distributed homogeneously.

Soares (2003) also stated that the Nusselt number (the ratio between convective to conductive heat transfers) in fully developed flow at the entrance region is continuously higher for the uniform wall heat flux. Also that the Nusselt number varies considerably in the entrance region because of the Impact of property deviation with temperature. Soares added that the inner-wall Nusselt number is moderately insensitive to the rheological behavior of the fluid.

According to Naikoti and Pagdipelli (2014) the influence of magnetic field parameter M on the dimensionless velocity profile F are inversely proportional to the temperature profiles. This impact is similar on both Newtonian and Non-Newtonian fluids. The temperature profiles increases with increase of slip parameter λ for both Newtonian and non-Newtonian fluids. The increase in power law index n causes a decrease in the dimensionless velocity and temperature profiles.

All these researches and others confirm that the fluid type and its flow pattern has a significant impact on the heat transfer profiles.

2.2 Effect of the annulus size and rotation of the drill string on the annular fluid flow.

As we are discussing the fluid flow through the annulus, one of the most important factors that interfere in our study is the size of the annular which can change many flow properties.
For example if the capacity of the annulus is small that will lead to the increase in the flow speed which we can conclude from the relationship governing the flow of any fluid in a restricted area

$Q=A.V.$

With lower A then that means increase in V because the amount of fluid flowing is not changing, with higher A that leads to lower V. Since the relationship between the fluid velocity and the flow time is directly proportional we can state that at lower area of the annulus the flow is expected to be at higher velocity and the flow type can change accordingly.

According to Bared (1990), the pressure loss resulting from the friction in the drilling process mostly assume that the drill string and annulus are a non-rotating system. Which is not true, since most of the time the drill string and annulus are at motion and rotating, due to the change in the fluid average velocity and apparent viscosity that changes the Reynolds number and fanning friction factor. Different researches found contradicting effects of drill-string rotation. Which can be due to the usage of different experimental conditions and different fluid properties.

According to the same research, there are two effects of drill string rotation on frictional pressure loss; firstly, rotation increases frictional pressure loss for low viscosity fluid due to the onset of centrifugal instabilities. Secondly, rotation decreases frictional pressure loss for high viscosity shear thinning fluid. Similarly, McCann et al. used a specially designed slim hole flow loop and found that rotation increases frictional pressure loss in turbulent flow, while rotation decreases frictional pressure loss in laminar flow. There were several studies where frictional pressure loss has been determined real field wells. These authors concluded that drill-string rotation increases the frictional pressure loss. On the contrary, Walker and Othmen conducted an experiment and found that frictional pressure loss decreases with increased drill-string rotation. They used a viscous shear thinning fluid and fairly narrow annuli, which the latter suppresses centrifugal instability.

2.3 Flow of Newtonian and Non-Newtonian Fluids in a Concentric Annulus with Rotation of the Inner Cylinder

As Nouri and Whitelaw (1997) discussed the flow of Newtonian and non-Newtonian fluids in a concentric annulus with rotation of the inner cylinder we will discuss their findings and compare it with the case that we are having in the annulus of the well.
Average velocity and resultant Reynolds shear stresses of both Newtonian and non-Newtonian fluids were measured in a fully developed concentric fluid flow with a diameter ratio of 0.5 at an inner cylinder rotational speed of 300 rpm.

With the fluids at laminar flow the rotation effects caused a steady increase in the drag coefficient by approximately 30 percent and skewed the average velocity with a narrow boundary near the inner wall at a thickness of 22 percent of gap between pipes.

These effects decreased gradually with bulk flow Reynolds number so that, in the turbulent flow region with a Rossby number 10, the drag coefficient and patterns of axial mean velocity with and without rotation were similar. The intensity of the turbulence quantities was enhanced by another study by Tong and Liu (2005) stated that the rheological properties of the fluid is a function of the rotation speed. Their research presented an exact solution for the unsteady rotational flow in an annular pipe. The equations they presented are based on the dynamic behavior of the fluid.

CHAPTER 3

METHODOLOGY

3.1 Governing equations

Most of the physical behaviors of any material are governed by equations. For this research some of the governing equations that will be used to simulate the flow of Non-Newtonian power law fluid will be

3.1.1 Momentum equation

Any mass that is moving with a certain velocity has a power. That power is called momentum.

For fluids the most relative and convenient equation to calculate the momentum is

$$\mathrm{\rho k}\left[\frac{\partial \mathrm{u}}{\partial \mathrm{t}} + U + \nabla U\right] = -k\nabla p + k\nabla \tau + k\mathrm{\rho g} \tag{3.1}$$

Momentum equation for flowing fluids

Where:

∇· is divergence, divergence is a vector operator that measures the magnitude of a vector field's source or sink at a given point
ρ is the amount of the quantity q per unit volume,
t is time,
σ is the generation of q per unit volume per unit time. Terms that generate ($\sigma > 0$) or remove ($\sigma < 0$) q are referred to as a "sources" and "sinks" respectively.
U is velocity
Tao is the deviatory stress tensor, The tensor relates a unit-length direction vector n to the stress vector T(n) across an imaginary surface perpendicular to n
K is the flow consistency index

Since the values of density and flow rate can be more convenient to obtain rather than the mass.

3.1.2 Continuity equation

For fluid flow simulation one of the most commonly used equations to express the flow is the continuity equation. Which is simply expressing the conservation of mass law for fluids.
It is simply describing the flow behavior in a conserved system.

$$\frac{\partial}{\partial t}(h) + \nabla(hU) = 0 \tag{3.2}$$

Continuity equation for fluids

Where

h.U is is the flux of q

h here is representing density

t is time

3.1.3 Power law equation

For Newtonian fluids many models are used to describe the relationship between stress and strain. One of these models is power law model. Which is represented by equation 3.3

$$\tau=K\ (\partial u/\partial y)^{n} \tag{3.3}$$

Power law equation

Where:

Tao here is stress

K is the flow consistency index (SI units Pa•sn),

$\partial u/\partial y$ is the shear rate or the velocity gradient perpendicular to the plane of shear (SI unit s−1), and

n is the flow behavior index (dimensionless).

3.1.4 Total energy equation (energy equation)

One of the most common equations in fluid dynamics that describes the conservation of energy in the system. Since the flow in this case is incompressible and the friction by viscous forces is negligible energy equation can be written as follows

$$\frac{\partial(\rho htot)}{\partial t} - \frac{\partial p}{\partial t} + \nabla.(\rho uhtot) = \nabla.(\gamma\nabla T) + \nabla.(U.\tau) + U.S_M \quad (3.4)$$

Total energy equation

Where

h_{tot} total enthalpy $=h+1/2\ U^2$

ρ is the density

v is velocity

z is the height of the flow

p is the pressure

$\partial p/\partial t$ change of pressure with time

$(U.\tau)$ work due to viscous stress

$U.S_M$ work due to external momentum sources

3.1.5 Heat transfer equations

This equation describes the process of heat transferring through any material. It is defined by the relationship between mass, specific heat and temperature difference in estimating the heat transfer through the material.

$$Q = m\ C_p\ \Delta t \quad (3.5)$$

Also From this equation describing the heat transfer for lengths inside fluid which is very similar to our case here in the annulus filled with fluid.

$$Q = \Delta t.K/L \quad (3.6)$$

Where

Q = quantity of energy transferred (kJ, Btu)

m = mass of substance (kg, lb)

C_p = specific heat of the substance (kJ/kgoC, kJ/kgoK, Btu/lb oF)

Δt = $(T_{in}-T_{out})$ temperature difference (rise or fall) in the substance (oC, K, oF)

K= heat capacity of the fluid

L= Length of the heat transfer distance (m,ft)

3.2. Research Methodology

The study will be conducted using the Computational Fluid Dynamics (CFD) approach, with ANSYS-CFX as the simulation software, where a CFD model will be created and validated against previous experimental data. The fluid will be modeled using Power Law model. A vertical wellbore is considered where the flow is assumed to be laminar and at steady state for developing the model.

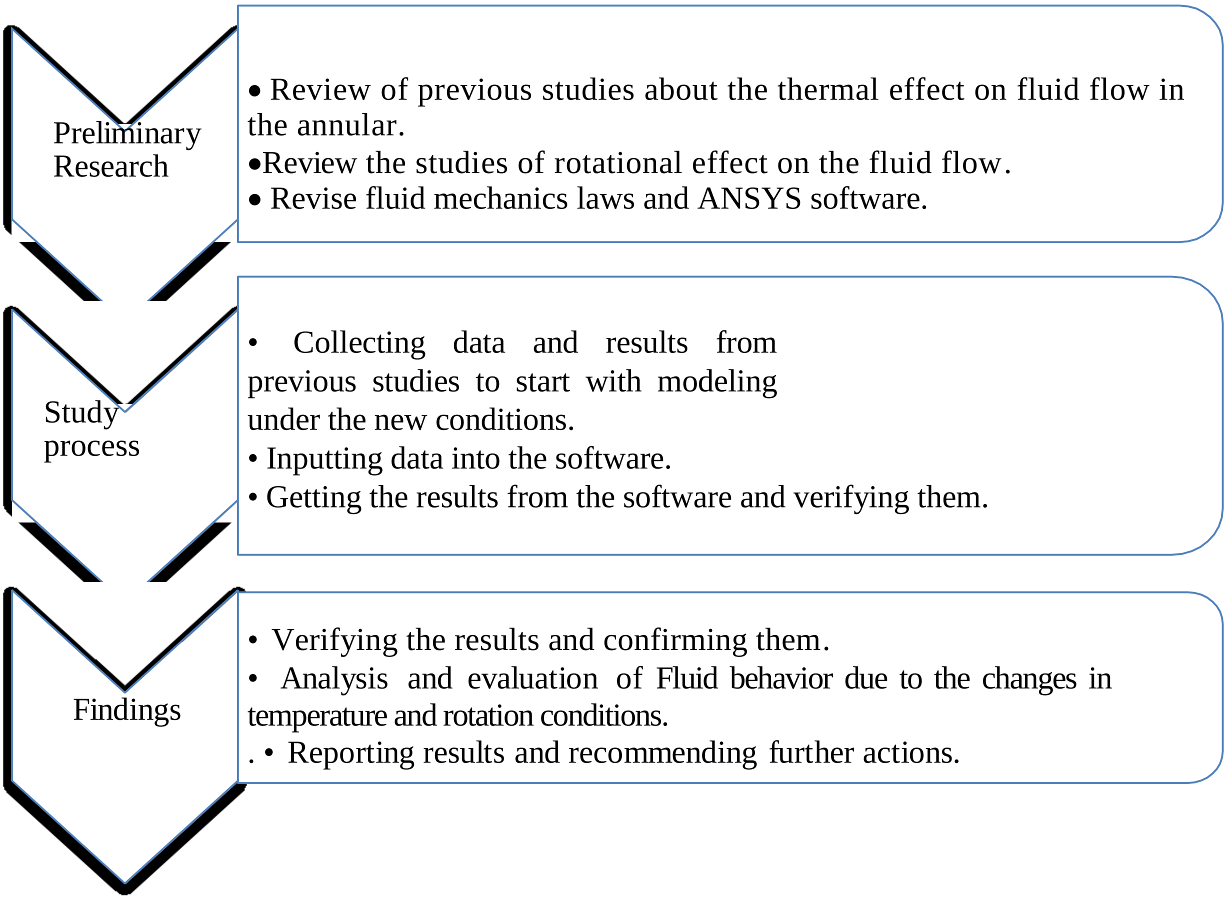

• Review of previous studies about the thermal effect on fluid flow in the annular.
•Review the studies of rotational effect on the fluid flow.
• Revise fluid mechanics laws and ANSYS software.

• Collecting data and results from previous studies to start with modeling under the new conditions.
• Inputting data into the software.
• Getting the results from the software and verifying them.

• Verifying the results and confirming them.
• Analysis and evaluation of Fluid behavior due to the changes in temperature and rotation conditions.
. • Reporting results and recommending further actions.

Figure 3.1: Flow chart of the project

3.2.1 Preliminary research

Early stages of this research similar previous studies were needed to get a better understanding about the topic. Researches and papers into the study of the rotation and thermal impact on the annular fluid flow were obtained through the available resources.

Different researches added new ideas and helped to understand the topic in a better way from various different angles. Most of the found researches were used as references to help achieving the objective of this research.

All the used data were mentioned properly in the reference part and cited in the literature review to maintain all the rights.

3.2.2 Benchmark identification

Due to our limitations regarding experimental studies which require sophisticated laboratory equipment and expensive materials. A benchmark experimental case study was preferred in this research.

After viewing several experimental studies and their relativity to the topic a thesis with the title “Flow of Newtonian and Non-Newtonian fluids in concentric and eccentric annuli” by Nouri (1993).

To accurately use the benchmark we need first to validate the model and match their outcome with the outcome we get from the same model with the same parameters for a velocity profile for example.

The starting point for the benchmark case will be the geometry static design.

3.2.3 Geometry static design

The dimensions of the annular tube is very essential in this study and can change the results dramatically. Hence the exact dimensions and parameters for the benchmark model will be used.

3.2.4 Meshing and grid independence study

After preparing the static model with the dimensions in table 3.1. Meshing type and size choice would be the next step to simulate the flow.

Trying two different types of meshing Tetrahedral and hexahedral. Hexahedral method was preferred for our case due to the shape of the annuli.

To choose the optimum element size and number of elements several simulation runs were tried and the optimum value was found.

3.2.5 Simulation validation

In order to confirm the model is similar to the one in the benchmark case we need to get the results from our model and then compare it with the results in the benchmark case model. In case of having a matching results, the benchmark and the model created are similar which means the simulation is validated.

3.2.6 Parametric studies and input simulation

The following step to preparing the model and validating it is to start making a study on the parameters Under study. Hence can know their impact on the fluid flowing.

3.2.7 Data analyzing and results

Getting the results of these studies can give the information needed to know the impact of heat transfer and rotation on the fluid flow achieving the purpose of this research.

3.3. Gantt Chart

The Gantt chart for Final Year Project I and Final Year Project II are shown in Table 3.1

Table 3.1 Gantt chart for FYP1 and FYP 2

Week	**1**	**2**	**3**	**4**	**5**	**6**	**7**	**8**	**9**	**10**	**11**	**12**	**13**	**14**
FYP 1 (Jan 2015)														
Studying the power law fluids And the ANSYS CFX software. Preparing benchmark study and working with the software.		🟩	🟩	🟩	🟩	🟩	🟩	🟩	🟩	🟩				
Parametric studies on the thermal effect on flow patterns					🟩	🟩	🟩	🟩	🟩					
Bench mark problem identification							🟩	🟩	🟩					
ANSYS CFX work for modeling and simulation of the benchmark case					🟩	🟩	🟩	🟩	🟩	🟩	🟩	🟩		
Model validation of the benchmark case										🟩	🟩	🟩	🟩	
Revising the benchmark results and interim report writing														🟩
FYP (May 2015)														
Results verification and modifying the simulation model.	🟦	🟦	🟦	🟦	🟦	🟦								
Further data analysis and reporting new updates for the study.								🟦	🟦	🟦	🟦	🟦		
Data collection & results analysis						🟦	🟦	🟦	🟦	🟦	🟦	🟦	🟦	
Finalizing the model and report writing													🟦	🟦

3.4 Key milestones of the project

Table 3.2 Key milestones

Project Key Milestones	Due
Bench mark problem identification and preparing for simulation validation	13th -20th April 2015
Complete Bench mark preparation for validation	6th -13th July 2015
Validation of simulation with the bench mark case	3rd august – 10th august 2015
Results analysis and data documentation	10th august -17th august 2015
Model finalizing and Oral presentation for discussion of the results	17th august -24th august 2015
Documenting the project and finalizing the final report	24th august-31st august 2015

3.5 Design of experiment

In the process of simulation the parameters that are being inspected are:-

1- Temperature
2- Rotation per minute
3- Flow behavior

Hence these conditions will be varied in different simulations and the resulting differences will be observed through extracting the resulting

1- Temperature transfer from outer wall to inner wall
2- Effect on dynamic viscosity
3- Pressure drop
4- Velocity profile

The simulations will be based on these input changes

Table 3.3: Design of experiment

RPM	Velocity (m/s)	Temp(at the hole wall) - K
0	0.1	298
		323
		373
		423
60	0.1	298
		323
		373
		423
120	0.1	298
		323
		373
		423
180	0.1	298
		323
		373
		423
220	0.1	298
		323
		373
		423

Comparing these outcomes should give an approximate overview regarding the effect of each parameter on these inspected results.

The resulting outcome should also be valuable for expecting the behavior of the fluid due to the change of the parameters mentioned above and help to improve the performance of the drilling fluid under the same conditions.

Applying statistics study to what could be the appropriate values for each trial the following table presents a good assumptions for the variable parameters assumed.

3.6 Static model

Establishing the benchmark static model using ANSYS-CFX with the following dimensions and parameters.

Table 3.4: Geometry design and flow properties

parameter	For concentric and laminar flow	
Outer Diameter (mm)	40.3	
Inner Diameter (mm)	20.1	
Bulk velocity U_b (m/s)	0.565	1.986
CMC temperature ^oC	25.0	
Density of CMC kg/m^3	1000	

Following the parameters shown in Table 3.4 resulted in this model shown in Figure 3.1

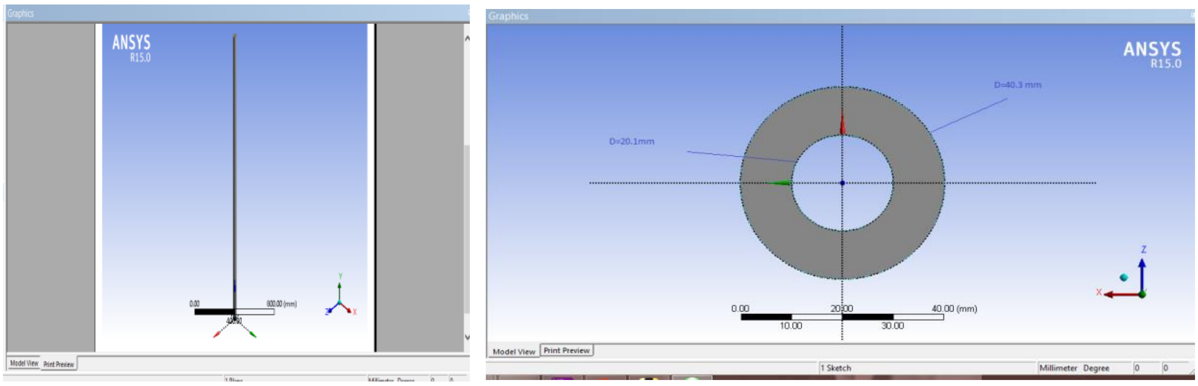

Figure 3.1 3D Static geometry model

3.7 Meshing and grid independence study

After creating the model we need to set our meshing and choose the suitable mesh grids size with the criteria and method explained in the methodology.

To choose the optimum element size and number of elements several simulation runs were tried and the optimum value was found at 20 mapped face meshing and 65 number of divisions with total number of 2067000 elements and 2171715 nodes.

Those values were found to be the mesh parameters that will get accurate results with the least possible time to run simulation.

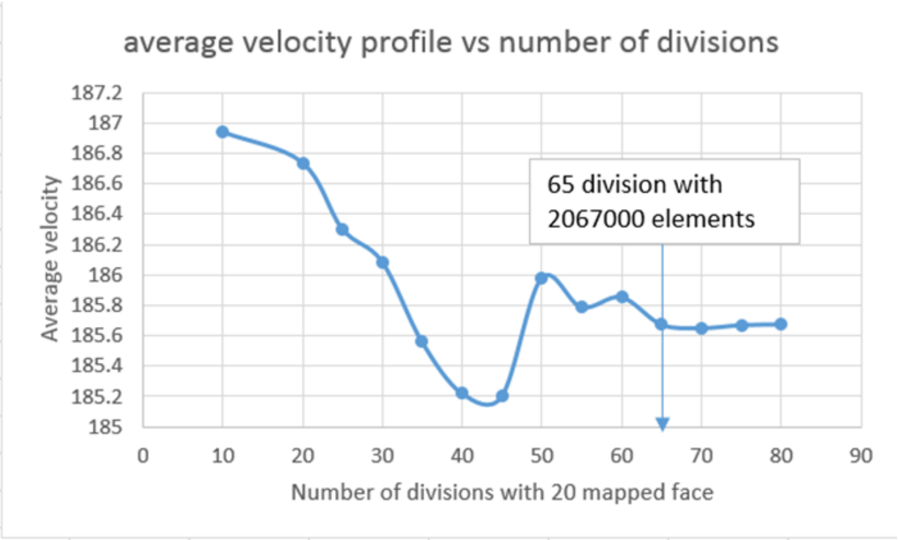

Figure 3.2 Grid independence study

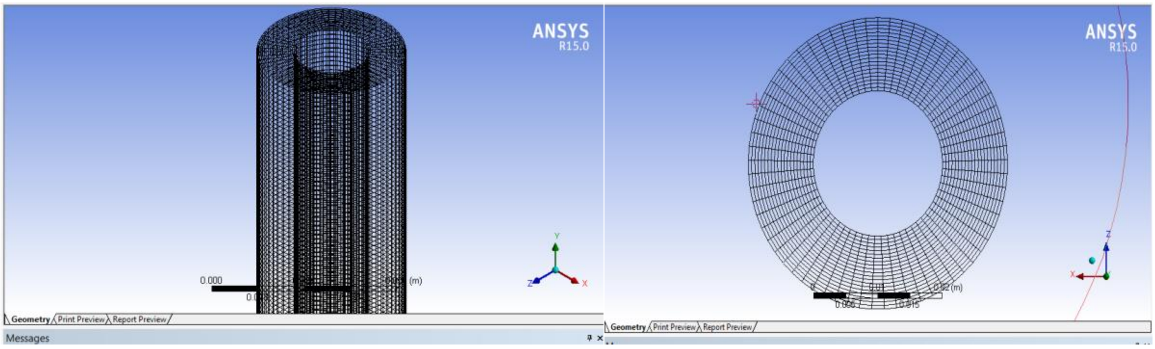

Figure 3.3 Meshed model vertical and horizontal view

4.3 Initial and boundary conditions

For this simulation, a specific velocity at the inlet was specified as 0.565 m/s and a zero gauge pressure defined at the outlet.

Also no slip boundary conditions were applied on both inner and outer walls. The material used was water with a density of 1000 kg/m3.

Table 3.5: Physics report and boundary conditions

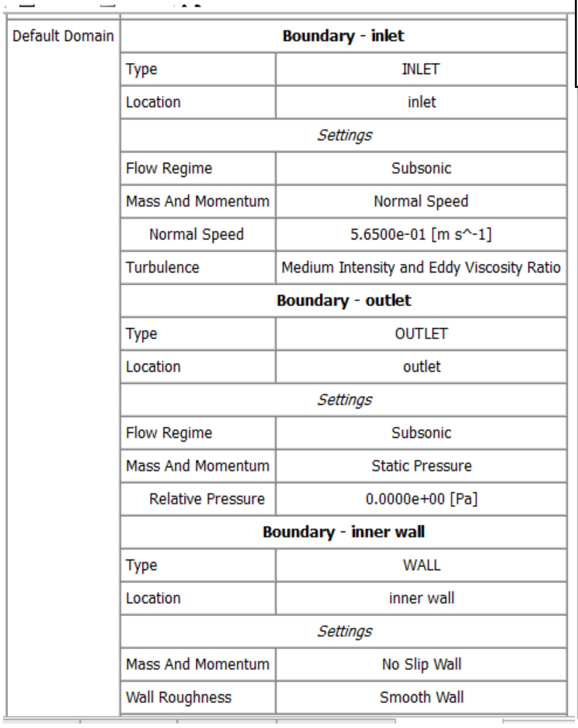

Default Domain	**Boundary - inlet**	
	Type	INLET
	Location	inlet
	Settings	
	Flow Regime	Subsonic
	Mass And Momentum	Normal Speed
	Normal Speed	5.6500e-01 [m s^-1]
	Turbulence	Medium Intensity and Eddy Viscosity Ratio
	Boundary - outlet	
	Type	OUTLET
	Location	outlet
	Settings	
	Flow Regime	Subsonic
	Mass And Momentum	Static Pressure
	Relative Pressure	0.0000e+00 [Pa]
	Boundary - inner wall	
	Type	WALL
	Location	inner wall
	Settings	
	Mass And Momentum	No Slip Wall
	Wall Roughness	Smooth Wall

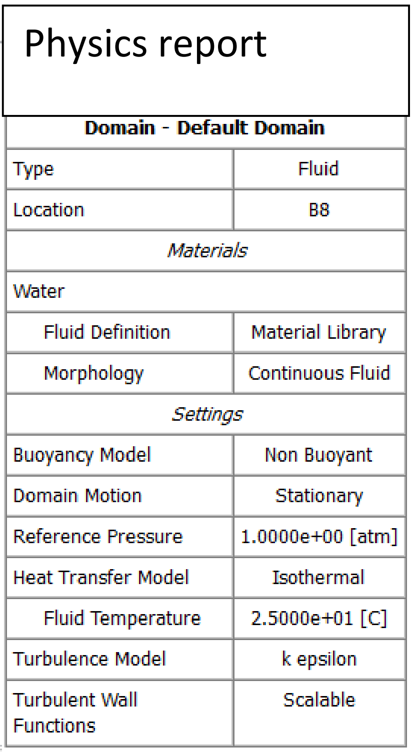

Physics report

Domain - Default Domain	
Type	Fluid
Location	B8
Materials	
Water	
Fluid Definition	Material Library
Morphology	Continuous Fluid
Settings	
Buoyancy Model	Non Buoyant
Domain Motion	Stationary
Reference Pressure	1.0000e+00 [atm]
Heat Transfer Model	Isothermal
Fluid Temperature	2.5000e+01 [C]
Turbulence Model	k epsilon
Turbulent Wall Functions	Scalable

CHAPTER 4

RESULTS AND DISCUSSION

4.1 Model validation

Running the model at the previous parameters resulted in the velocity profile results in table 4.2 as well as the results of processing these data to get the same table as in the bench mark study.

Table 4.1: Velocities and location results and normalized results

[Data]			
Velocity [m s^-1]	X [m]	$(r-R_1)/(R_2-R_1)$	u/U_b
0.00E+00	2.01E-02	1.00E+00	0
1.63E-01	1.96E-02	9.50E-01	0.288742674
3.03E-01	1.91E-02	9.00E-01	0.537041225
4.25E-01	1.86E-02	8.50E-01	0.753015437
5.29E-01	1.81E-02	8.00E-01	0.936941446
6.16E-01	1.76E-02	7.50E-01	1.089600651
6.85E-01	1.71E-02	7.00E-01	1.212000004
7.38E-01	1.66E-02	6.50E-01	1.305377694
7.75E-01	1.61E-02	6.00E-01	1.371275745
7.98E-01	1.56E-02	5.50E-01	1.411724828
8.08E-01	1.51E-02	5.00E-01	1.429825651
8.09E-01	1.46E-02	4.50E-01	1.432229777
8.03E-01	1.41E-02	4.00E-01	1.421474145
7.84E-01	1.36E-02	3.50E-01	1.38753737
7.48E-01	1.31E-02	3.00E-01	1.324186177
6.93E-01	1.26E-02	2.50E-01	1.225972175
3.77E-01	1.11E-02	1.00E-01	0.667488312
2.11E-01	1.05E-02	5.00E-02	0.374229319
0.00E+00	1.00E-02	0.00E+00	0

Plotting the normalized results to compare with the plot from our benchmark study.

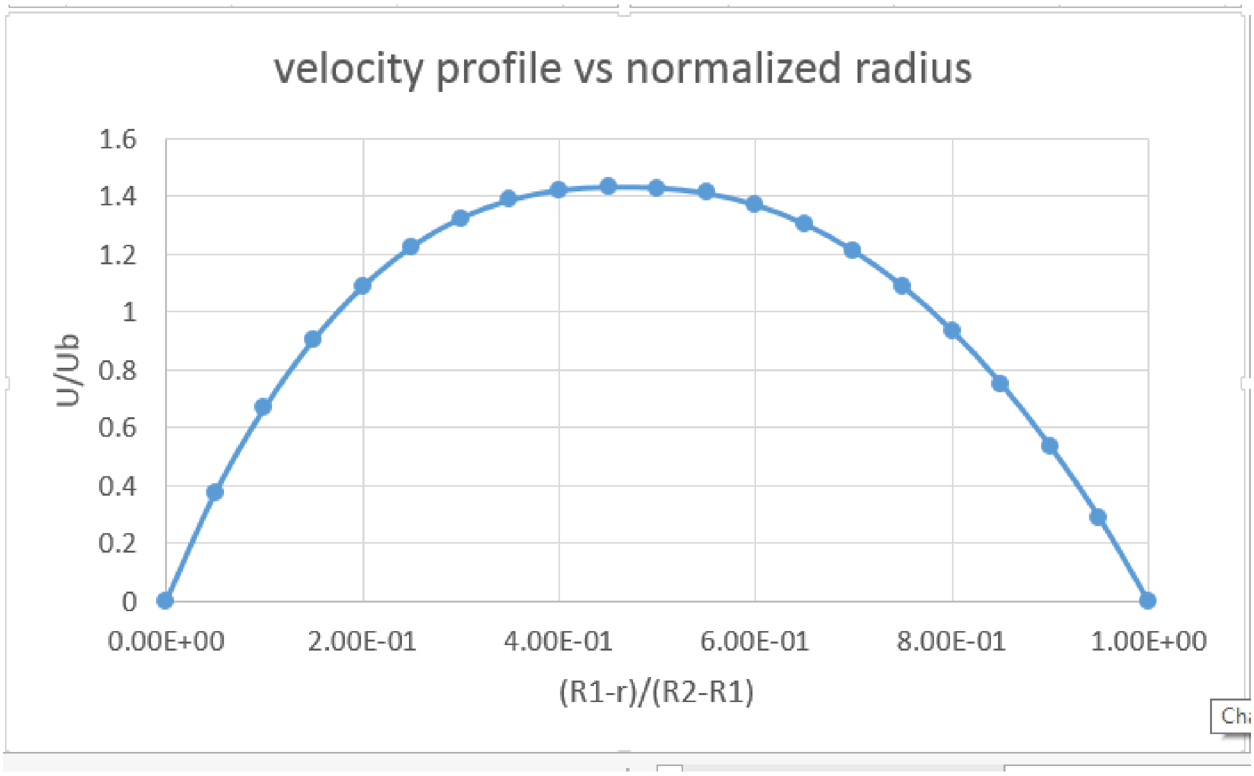

Figure 4.5 Velocity profile vs normalized results

Digitizing the results for the plot from the benchmark study and plotting them against the results from the new model will result in Figure 4.6. The blue dots are representing the digitized benchmark data and the orange line is representing the new model.

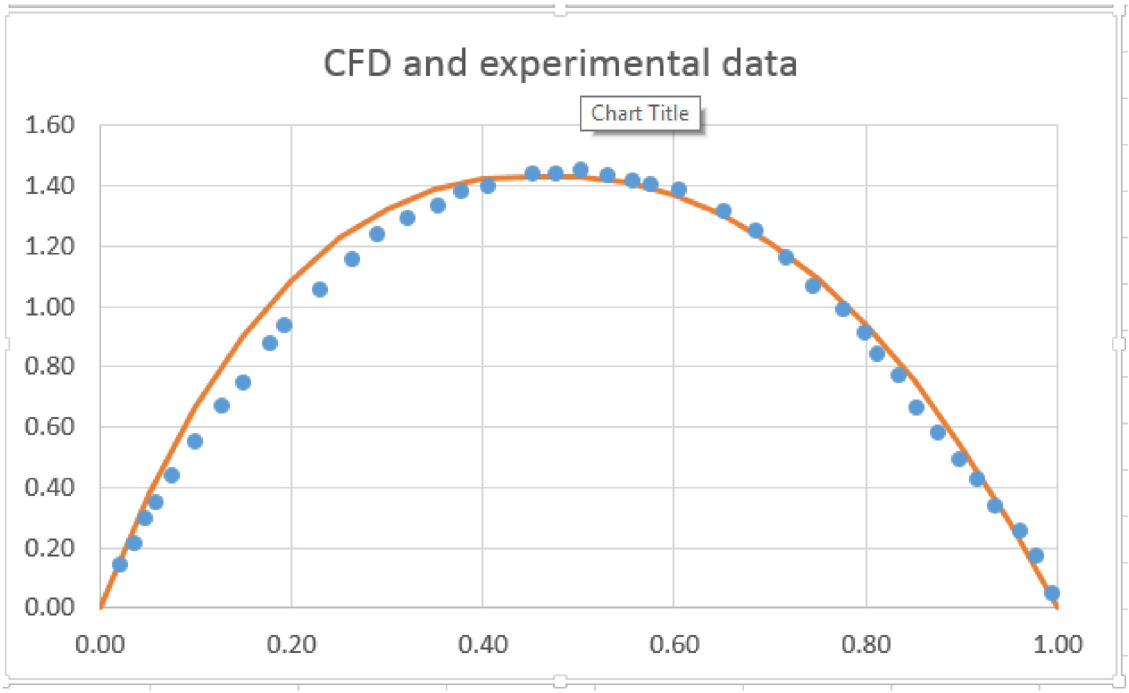

Figure 4.5 Digitized results from the benchmark study vs the new model results

As seen from the graph the two results are closely similar. This concludes that the new model is validated against the benchmark case study.

As the model is validated now changing the parameters under inspection and viewing the results is the following process.

4.6 Parametric changes results

Applying the different parameters according to the design of experiment table mentioned in the methodology the results are plotted and extracted on the plane across the annulus showing the following :-

1- Temperature transfer from the outer wall to the inner wall.
2- Dynamic viscosity change at different temperature and different rotation speeds.
3- Pressure drop at different parameters.
4- Velocity profiles at different conditions.

Since simulation runs consume prolonged time the available results for comparison are limited, however showing the expectations of the behavior of the fluid at different conditions.

4.6.1 Temperature transfer

Fixing the rotation at 0 RPM and changing the temperature shows that similar behavior through the annulus is taking place in all cases. The temperature starts transferring through the fluid starting from the outer wall at highest temperature dropping to the inner wall temperature which is 298 K.

However when RPM is introduced the results are changing.

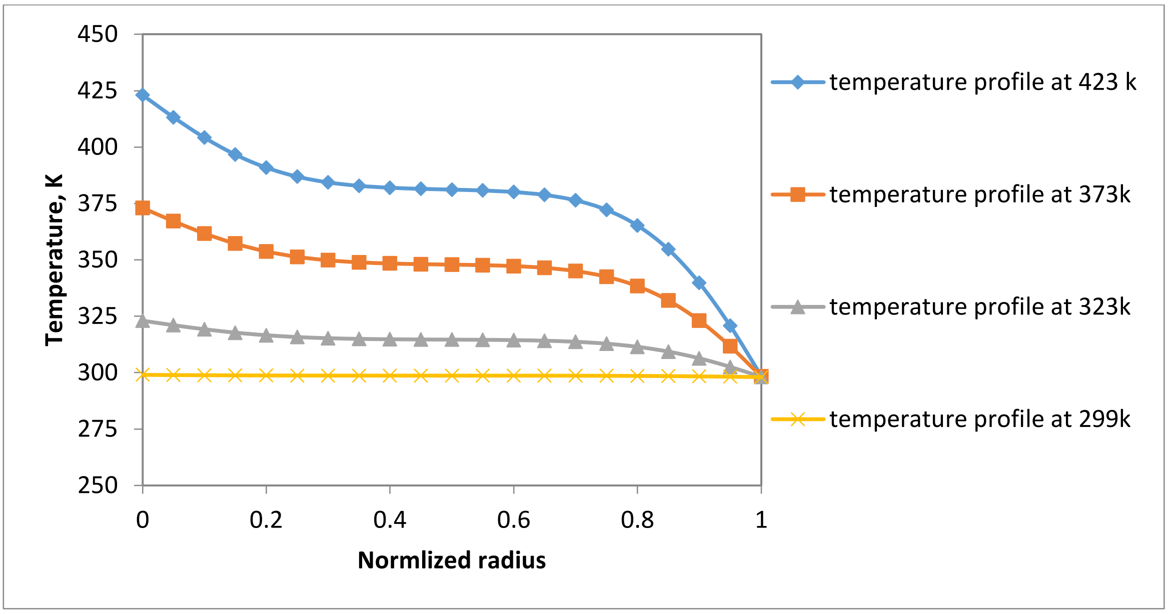

Figure 4.6 Temperature profiles at 0 RPM and different temperature

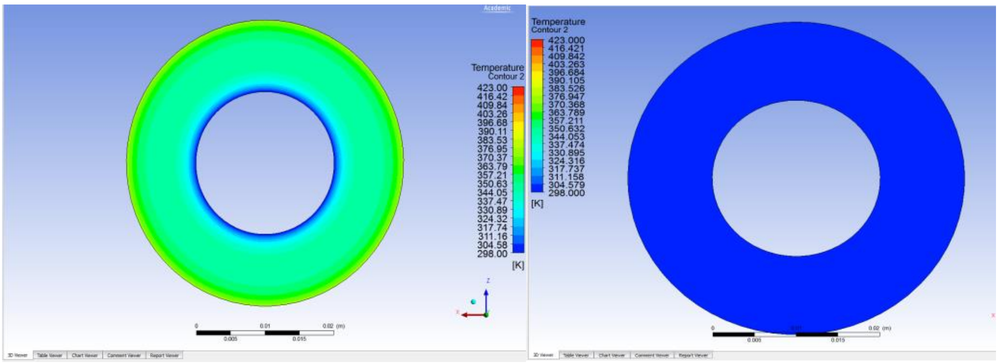

Figure 4.7 Contour profile at 0 RPM at temperature 373 K and 299 K

As the contour profiles show us in the case of higher temperature at the wall with no rotation the temperature is transferred through the annulus with high decrease towards the center. However this distribution rate will be different with higher RPM as shown in the figure 4.9

While in the previous case the heat transfer profile remains relatively similar when RPM is increases we notice change in the heat transfer profile. Closer to the outer wall the temperature at static condition is higher than at 220RPM and at 220 the temperature is dropping faster than at static condition. However in the middle of the annulus both profiles seem symmetric and moving at same rate.

Near the rotation the temperature is dropping slower at 220 RPM due to the turbulent condition that helps to distribute the heat, unlike the case in static conditions.

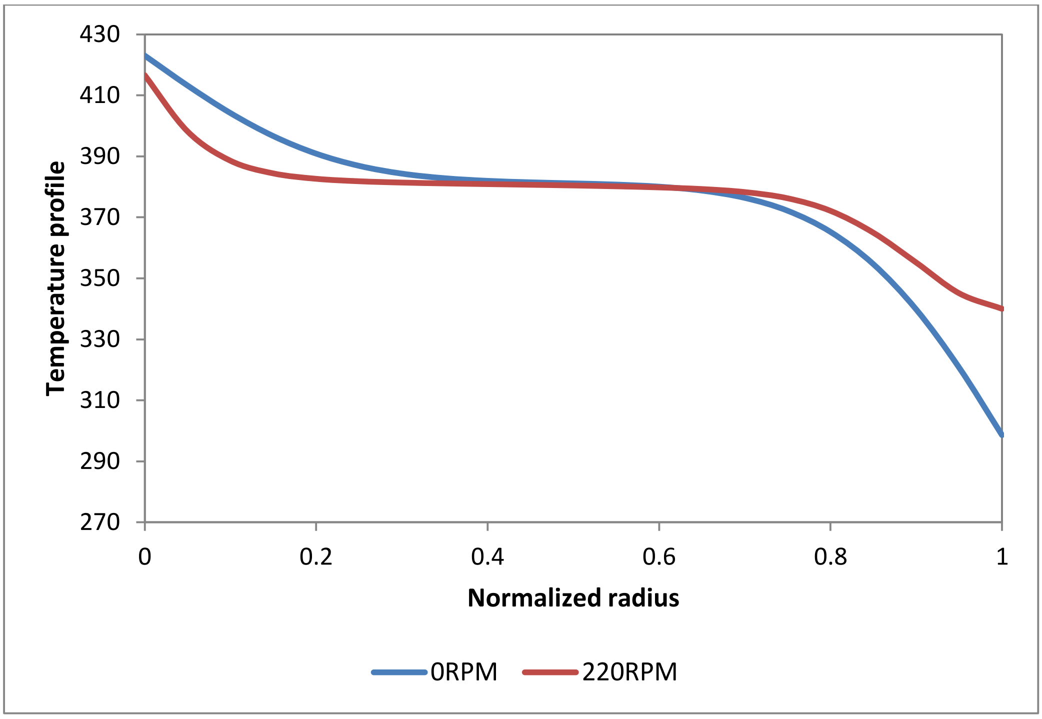

Figure 4.8 Temperature profiles at same temperature and different RPM

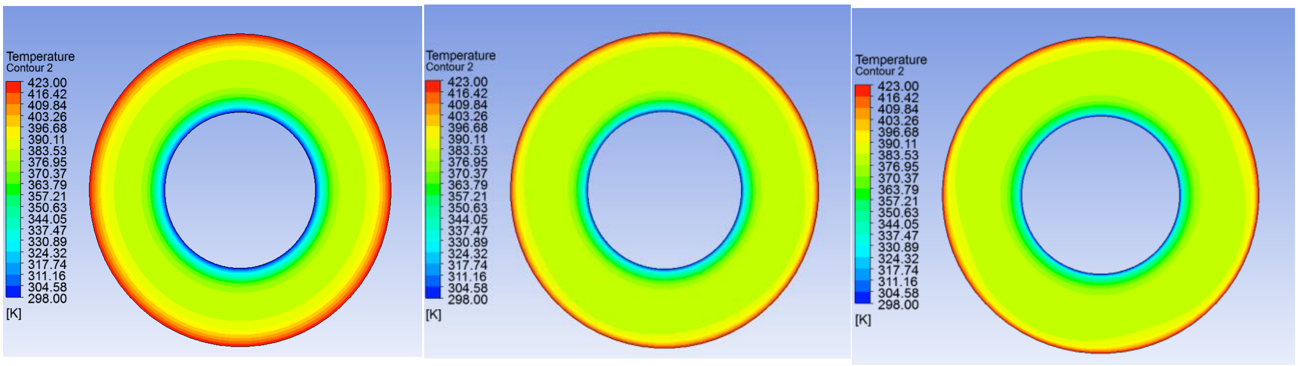

Figure 4.9 Contour profile at 423K at 0 RPM and 120 RPM and 220 RPM

As shown in the contour profiles we notice the different rotation speed is causing different distribution of heat in the annulus. The distribution is at lowest at 0 RPM and highest at 220 RPM.

This is also impacting the dynamic viscosity and hence coupled velocity.

4.6.2 Dynamic viscosity

The dynamic viscosity profile was recorded at both changing temperature and changing RPM. The results suggest that changing the temperature doesn't impact dynamic viscosity to a significant value, nonetheless changing the RPM decrease dynamic viscosity near the drill string. That effect explains the increase in velocity near the drill string due to decrease in viscosity.

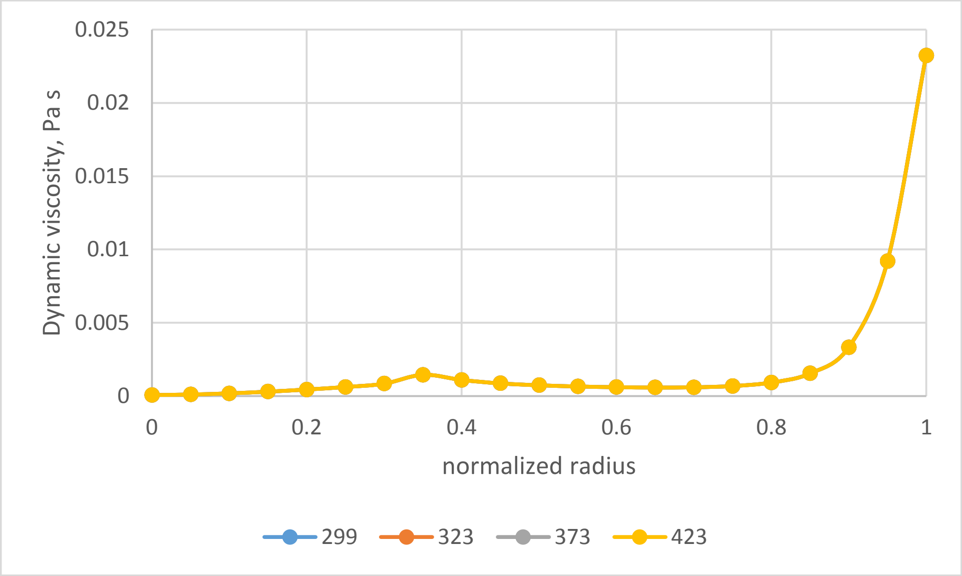

Figure 4.10 Dynamic viscosities at same RPM and different temperatures

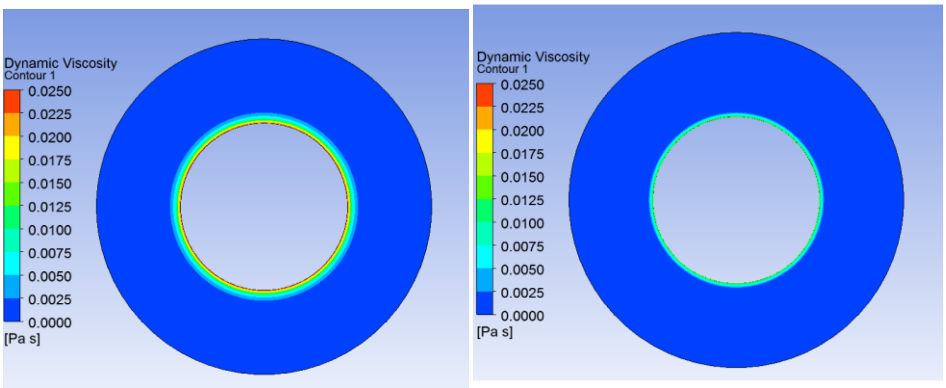

Figure 4.11 Contour profiles of dynamic viscosity at 0 RPM and 220 RPM

The contour profile shows as well that the dynamic viscosity near the drill string is decreasing with increase in rotation.

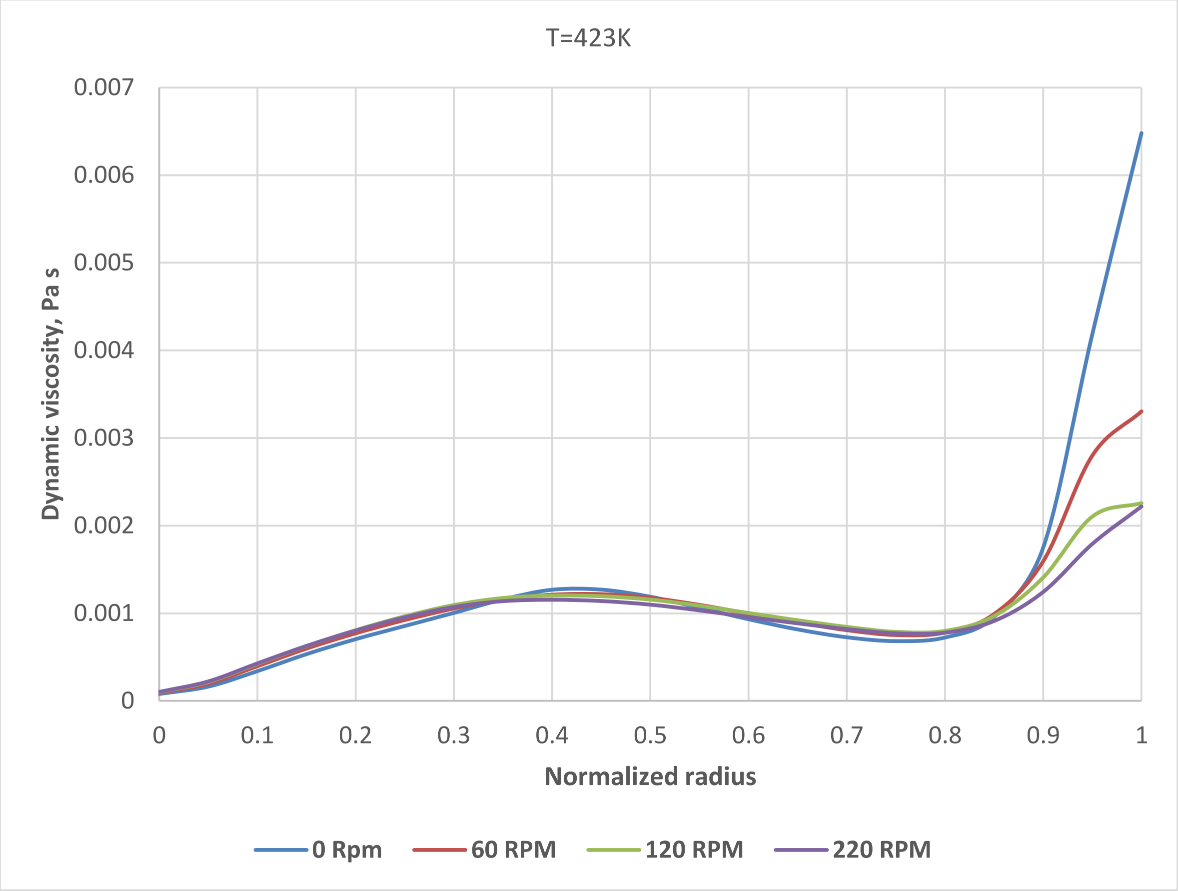

Figure 4.12 Dynamic viscosities at different RPM and same temperature

4.6.3 Pressure drop

Taking pressure drop in consideration at different temperatures and RPMs no results show a significant change in pressure drop due to neither temperature nor RPM changing. The pressure drop profile remained constant through different RPMs and temperatures. In fact several research tried explaining the direct relation between rotation and pressure drop, yet different theories were introduced. The most common theory is the secondary flow effect which causes decrease in the pressure drop at low RPM yet with increase in RPM the secondary flow area becomes larger and the pressure drop returns to normal levels.

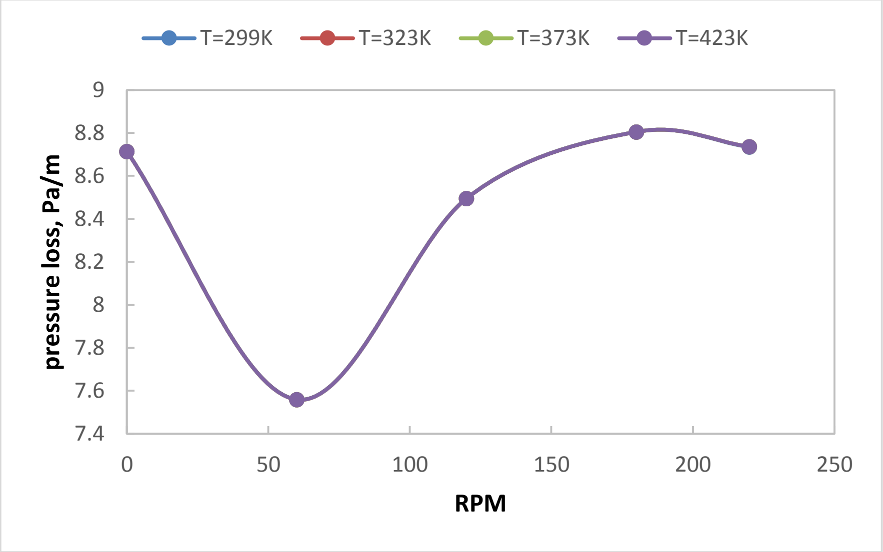

Figure 4.13 Pressure drop profile at different RPM and different temperature

4.6.4 Velocity profiles

What is noticed in that the change occurring is irrelevant of temperature and the main cause of this shift is RPM. Near the drill string there is a rapid and sudden increase in the velocity.

The similarity between the turning point in velocity profile and dynamic viscosity profile provide an explanation. Due to the decrease in dynamic viscosity resulting from RPM steering of the fluid, the velocity is increased.

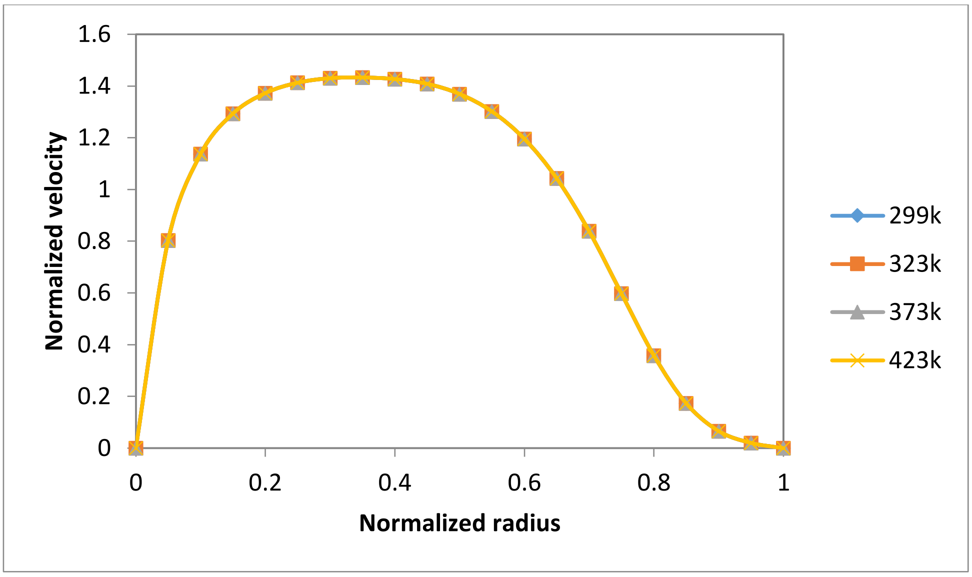

Figure 4.14 Velocity profiles at different temperature and same RPM

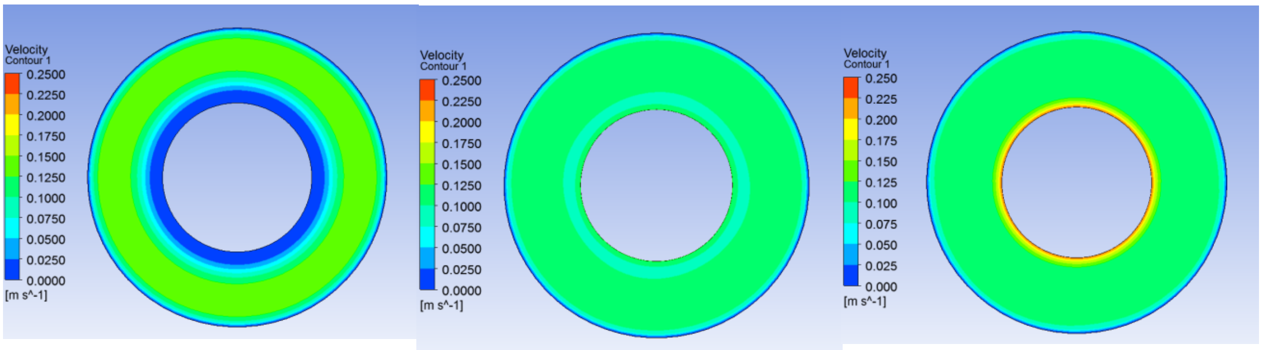

Figure 4.15 Contour profiles of velocity at 0 RPM 120 RPM and 220 RPM

As shown in the contour profiles the velocity is increasing throughout the annulus with increase of rotation and increasing significantly around the drill string.

This significant increase can be crucial in understanding cutting transportation in such condition. Combined with dynamic viscosity change we can have a picture of how the cutting will be transported through this fluid at different rotations in the drilling process and we can control the cutting transportation by changing the RPM.

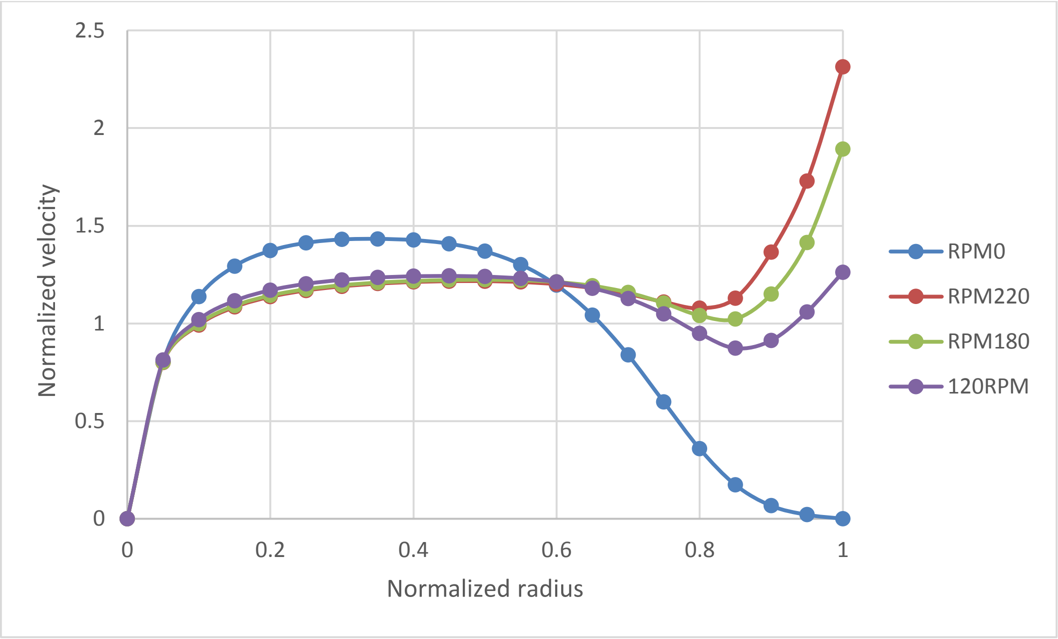

Figure 4.16 Velocity profiles at different RPM and fixed temperature

CHAPTER 5

CONCLUSION AND RECOMMENDATION

The study has reviewed the fluid flow profile in the annular of the well. The study was focusing on the behavior of the fluid flow as a function of temperature. In addition to the thermal effect there is also the rotation effect which was considered as a factor in changing the behavior of the fluid flow.

Through the study the results were taken from previous confirmed experiments and the simulation was operated on the ANSYS-CFX by CFD simulation. The results were validated and verified by the software. Models were performed on the software for better understanding of the changes in the fluid flow.

The results has shown that temperature has less impact than expected, however it has shown the huge impact of the RPM on the dynamic viscosity ,velocity , temperature distribution as well as the pressure drop.

These findings can be significant in high temperature wells, since it is helping us expect the behavior of the fluid under different rotation speeds.

The recommendations that this study can offer are continuing to study more parameters impact on the flow of Non-Newtonian fluids in annuli, since it was noticed that any minor change in any parameter can result in entirely different results on both the fluid flow pattern and its rheological properties. This study also suggests adding the flow rate in consideration as a parameter that is affecting the fluid behavior.

This study will help for opening new doors to better anticipation of the Non-Newtonian fluids flow under very specific conditions and environment. The results that this study is presenting lead to better understanding of the mud behavior and further researches might be able to present a better performing drilling fluid components for these conditions in particular to ensure better performance and avoiding the suggested behavioral disorders in the mud flow pattern.

REFERENCES

Bared, S. (1990). "Another Method Depicting the Effect of Rotation of Drilling Fluids in a Pipe on the Pressure Drop."

Bataller, R. C. (2007). "Viscoelastic fluid flow and heat transfer over a stretching sheet under the effects of a non-uniform heat source, viscous dissipation and thermal radiation." International Journal of Heat and Mass Transfer 50(15): 3152-3162.

Cho, Y. and J. P. Harnett (1982). "Non-Newtonian fluids in circular pipe flow." Advances in heat transfer 15: 59-141.

Dodge, D. and A. Metzner (1959). "Turbulent flow of non-Newtonian systems." AIChE Journal 5(2): 189-204.

Escudier, M., et al. (2002). "Fully developed laminar flow of purely viscous non-Newtonian liquids through annuli, including the effects of eccentricity and inner-cylinder rotation." International Journal of Heat and Fluid Flow 23(1): 52-73.

Fang, P., et al. (1999). "Characteristics of laminar viscous shear-thinning fluid flows in eccentric annular channels." Journal of non-newtonian fluid mechanics 84(1): 1-17.

Guckes, T. (1975). "Laminar flow of non-newtonian fluids in an eccentric annulus." Journal of Manufacturing Science and Engineering 97(2): 498-506.

Haciislamoglu, M. and J. Langlinais (1990). "Non-Newtonian flow in eccentric annuli." Journal of Energy Resources Technology 112(3): 163-169.

Holdsworth, S. (1971). "Applicability of rheological models to the interpretation of flow and processing behaviour of fluid food products." Journal of Texture Studies 2(4): 393-418.

Ikoku, C. U. and H. J. Ramey (1978). Transient flow of non-Newtonian power-law fluids in porous media, Dept. of Energy.

Karwe, M. V. and Y. Jaluria (1990). "Numerical simulation of fluid flow and heat transfer in a single-screw extruder for non-Newtonian fluids." Numerical heat transfer 17(2): 167-190.

Kays, W. and E. Leung (1963). "Heat transfer in annular passages—hydrodynamically developed turbulent flow with arbitrarily prescribed heat flux." International Journal of Heat and Mass Transfer 6(7): 537-557.

Dunn, J.E., K.R. Rajagopal, Fluids of differential type: critical review and thermodynamic analysis, Int. J. Eng. Sci. 33 (5) (1995) 689–729.

Manglik, R. and P. Fang (2002). "Thermal processing of viscous non-Newtonian fluids in annular ducts: effects of power-law rheology, duct eccentricity, and thermal boundary conditions." International Journal of Heat and Mass Transfer 45(4): 803-814.

Metzner, A. (1965). "Heat transfer in non-Newtonian fluids." Advances in heat transfer 2: 357-397.

Naikoti, K., & Pagdipelli, K. (2014). Effects of heat source/sink on MHD flow and heat transfer of a non-Newtonian power-law fluid on a stretching surface with thermal radiation and slip-conditions. Thermal Science, (00), 35-35.

Nouri, J. and J. Whitelaw (1997). "Flow of Newtonian and non-Newtonian fluids in an eccentric annulus with rotation of the inner cylinder." International Journal of Heat and Fluid Flow 18(2): 236-246.

Parmentier, E. (1978). "A study of thermal convection in non-Newtonian fluids." Journal of Fluid Mechanics 84(01): 1-11.

Soares, E. J., et al. (2003). "Heat transfer to viscoplastic materials flowing axially through concentric annuli." International Journal of Heat and Fluid Flow **24** (5): 762-773.

Soliman, M., et al. (1968). "A general heat transfer correlation for annular flow condensation." Journal of Heat Transfer 90(2): 267-274.

Tong, D. and Y. Liu (2005). "Exact solutions for the unsteady rotational flow of non-Newtonian fluid in an annular pipe." International journal of engineering science 43(3): 281-289.

Tong, D., et al. (2005). "Exact solutions for the flow of non-Newtonian fluid with fractional derivative in an annular pipe." Science in China Series G: Physics, Mechanics and Astronomy 48(4): 485-495.

Turian, R. M. and R. Byron Bird (1963). "Viscous heating in the cone-and-plate viscometer—II: Newtonian fluids with temperature-dependent viscosity and thermal conductivity." Chemical Engineering Science 18(11): 689-696.

APPENDICES

Appendix 1

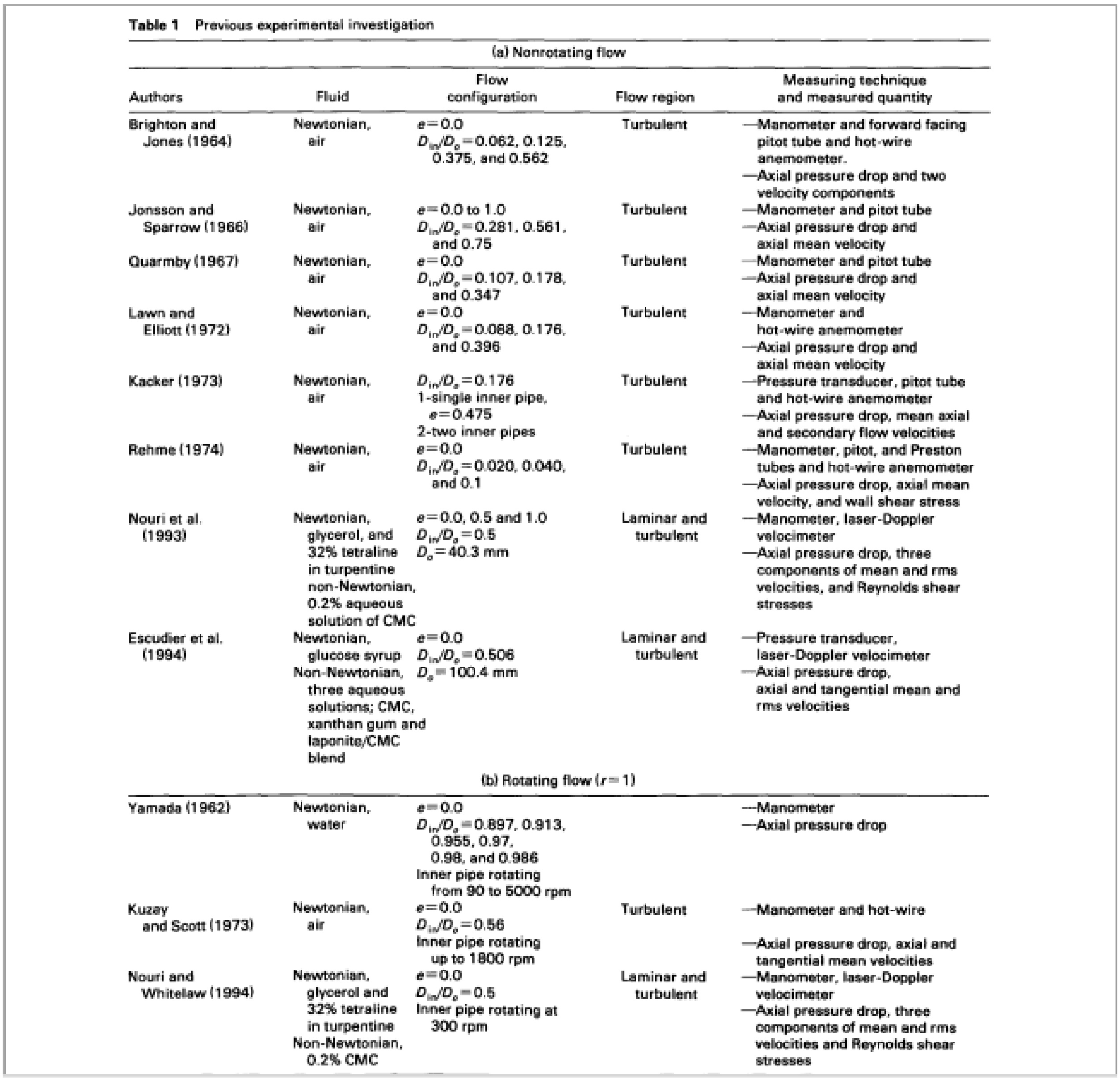

Table 1 Previous experimental investigation

Authors	Fluid	Flow configuration	Flow region	Measuring technique and measured quantity
		(a) Nonrotating flow		
Brighton and Jones (1964)	Newtonian, air	$e=0.0$ $D_{in}/D_o=0.062$, 0.125, 0.375, and 0.562	Turbulent	—Manometer and forward facing pitot tube and hot-wire anemometer. —Axial pressure drop and two velocity components
Jonsson and Sparrow (1966)	Newtonian, air	$e=0.0$ to 1.0 $D_{in}/D_o=0.281$, 0.561, and 0.75	Turbulent	—Manometer and pitot tube —Axial pressure drop and axial mean velocity
Quarmby (1967)	Newtonian, air	$e=0.0$ $D_{in}/D_o=0.107$, 0.178, and 0.347	Turbulent	—Manometer and pitot tube —Axial pressure drop and axial mean velocity
Lawn and Elliott (1972)	Newtonian, air	$e=0.0$ $D_{in}/D_o=0.088$, 0.176, and 0.396	Turbulent	—Manometer and hot-wire anemometer —Axial pressure drop and axial mean velocity
Kacker (1973)	Newtonian, air	$D_{in}/D_o=0.176$ 1-single inner pipe, $e=0.475$ 2-two inner pipes	Turbulent	—Pressure transducer, pitot tube and hot-wire anemometer —Axial pressure drop, mean axial and secondary flow velocities
Rehme (1974)	Newtonian, air	$e=0.0$ $D_{in}/D_o=0.020$, 0.040, and 0.1	Turbulent	—Manometer, pitot, and Preston tubes and hot-wire anemometer —Axial pressure drop, axial mean velocity, and wall shear stress
Nouri et al. (1993)	Newtonian, glycerol, and 32% tetraline in turpentine non-Newtonian, 0.2% aqueous solution of CMC	$e=0.0$, 0.5 and 1.0 $D_{in}/D_o=0.5$ $D_o=40.3$ mm	Laminar and turbulent	—Manometer, laser-Doppler velocimeter —Axial pressure drop, three components of mean and rms velocities, and Reynolds shear stresses
Escudier et al. (1994)	Newtonian, glucose syrup Non-Newtonian, three aqueous solutions; CMC, xanthan gum and laponite/CMC blend	$e=0.0$ $D_{in}/D_o=0.506$ $D_o=100.4$ mm	Laminar and turbulent	—Pressure transducer, laser-Doppler velocimeter —Axial pressure drop, axial and tangential mean and rms velocities
		(b) Rotating flow ($r=1$)		
Yamada (1962)	Newtonian, water	$e=0.0$ $D_{in}/D_o=0.897$, 0.913, 0.955, 0.97, 0.98, and 0.986 Inner pipe rotating from 90 to 5000 rpm		—Manometer —Axial pressure drop
Kuzay and Scott (1973)	Newtonian, air	$e=0.0$ $D_{in}/D_o=0.56$ Inner pipe rotating up to 1800 rpm	Turbulent	—Manometer and hot-wire —Axial pressure drop, axial and tangential mean velocities
Nouri and Whitelaw (1994)	Newtonian, glycerol and 32% tetraline in turpentine Non-Newtonian, 0.2% CMC	$e=0.0$ $D_{in}/D_o=0.5$ Inner pipe rotating at 300 rpm	Laminar and turbulent	—Manometer, laser-Doppler velocimeter —Axial pressure drop, three components of mean and rms velocities and Reynolds shear stresses

Appendix 2

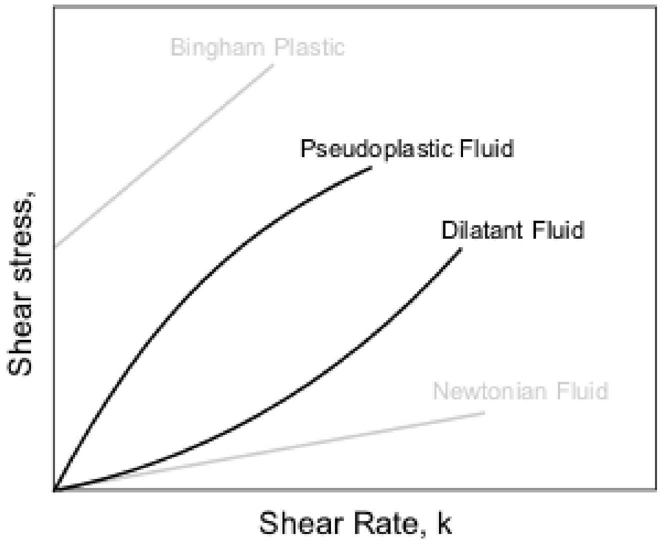

Appendix 3

Table 1 - Reduced Velocity Profile for a Power-law Fluid

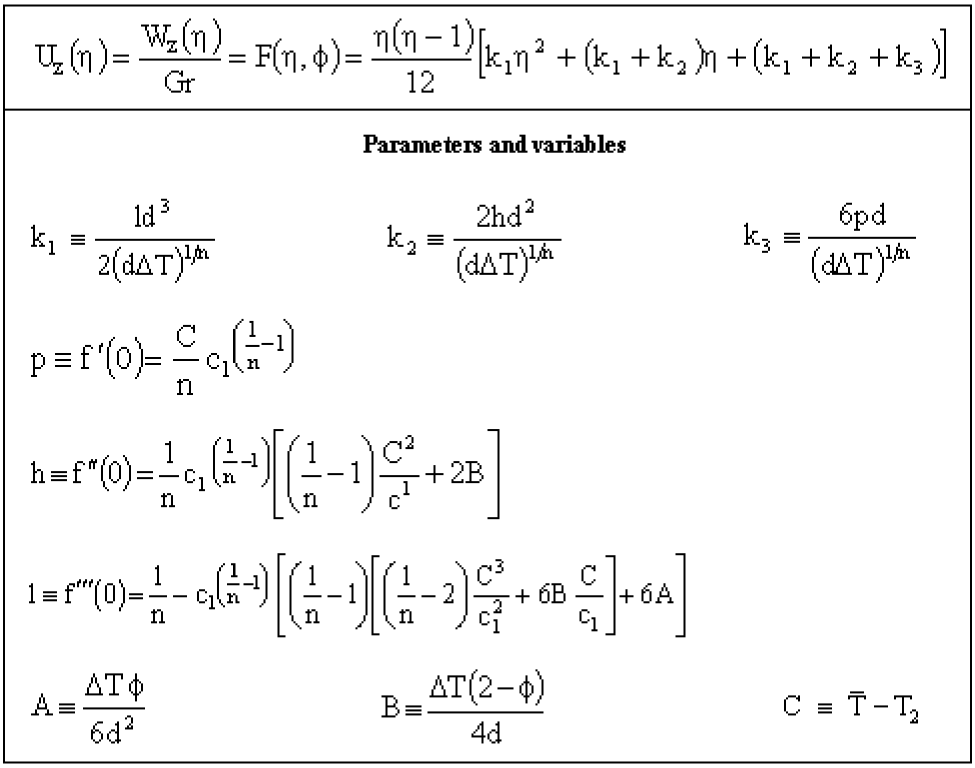

$$U_z(\eta) = \frac{W_z(\eta)}{Gr} = F(\eta, \phi) = \frac{\eta(\eta - 1)}{12}\left[k_1\eta^2 + (k_1 + k_2)\eta + (k_1 + k_2 + k_3)\right]$$

Parameters and variables

$$k_1 \equiv \frac{ld^3}{2(d\Delta T)^{1/n}} \qquad k_2 \equiv \frac{2hd^2}{(d\Delta T)^{1/n}} \qquad k_3 \equiv \frac{6pd}{(d\Delta T)^{1/n}}$$

$$p \equiv f'(0) = \frac{C}{n} c_1^{\left(\frac{1}{n}-1\right)}$$

$$h \equiv f''(0) = \frac{1}{n} c_1^{\left(\frac{1}{n}-1\right)}\left[\left(\frac{1}{n} - 1\right)\frac{C^2}{c^1} + 2B\right]$$

$$l \equiv f'''(0) = \frac{1}{n} - c_1^{\left(\frac{1}{n}-1\right)}\left[\left(\frac{1}{n} - 1\right)\left[\left(\frac{1}{n} - 2\right)\frac{C^3}{c_1^2} + 6B\,\frac{C}{c_1}\right] + 6A\right]$$

$$A \equiv \frac{\Delta T \phi}{6d^2} \qquad B \equiv \frac{\Delta T(2 - \phi)}{4d} \qquad C \equiv \bar{T} - T_2$$